Published in final edited form as:

J Immunol. 2007 December 15; 179(12): 8042–8050.

Passive Immunization against the MHC Class I Molecule Mamu-AG Disrupts Rhesus Placental Development and Endometrial Responses[1]

Gennadiy I. Bondarenko[*], **David W. Burleigh**[*,2], **Maureen Durning**[*], **Edith E. Breburda**[*], **Richard L. Grendell**[*], and **Thaddeus G. Golos**[3,*,†]

[*]Wisconsin National Primate Research Center, University of Wisconsin School of Medicine and Public Health, University of Wisconsin, Madison, WI 53715

[†]Department of Obstetrics and Gynecology, University of Wisconsin School of Medicine and Public Health, University of Wisconsin, Madison, WI 53715

Abstract

The unique MHC phenotype of the human and nonhuman primate placenta has suggested a potential role in maternal-fetal immune tolerance, pregnancy success, and maternal as well as fetal well-being. In the rhesus monkey (*Macaca mulatta*) a non-classical MHC class I molecule, Mamu-AG, is a putative homologue of HLA-G and is hypothesized to play a role in maternal-fetal immune interactions during pregnancy. Rhesus monkeys were passively immunized during the second week after implantation with a mAb against Mamu-AG. Passive immunization altered the growth and vascularization of the fetal placenta, the placental modification of maternal endometrial vessels, the maternal leukocyte response to implantation, and the differentiation of epithelial and stromal cells in the endometrium. These data are the first to demonstrate in vivo the importance of MHC class I molecules expressed on primate trophoblasts in establishing an important environment for pregnancy success through coordinated interactions between endometrial and fetal tissues.

The polymorphism of classical MHC class I molecules is critical to the surveillance function of an intact immune system. In contrast to the highly polymorphic, classical MHC class I molecules (HLA-A, -B, and -C), the nonclassical human MHC class I gene products (HLA-E, -F, and -G) exhibit extremely limited polymorphism. HLA-G has a novel expression pattern in invasive extravillous placental trophoblasts that migrate into the maternal endometrium at implantation (1–3), and it has been implicated in the regulation of the maternal immune response to pregnancy. HLA-G is complexed with β_2-microglobulin (4), recognized by $CD8^+$ cells (5), and binds the same array of peptides as classical HLA

---

[1]This work was supported by National Institutes of Health Grants HD37120 and HD34215 (to T.G.G.), and RR000167 (to Wisconsin National Primate Research Center).

[3]Address correspondence and reprint requests to Dr. Thaddeus G. Golos, Wisconsin National Primate Research Center, University of Wisconsin, 1223 Capitol Court, Madison, WI 53715. golos@primate.wisc.edu.

[2]Current Address: Division of Natural Sciences and Mathematics, Richard Stockton College of New Jersey, Pomona, NJ 08240.

Disclosures

The authors have no financial conflict of interest.

molecules (6, 7). HLA-G has been proposed to play important roles in the regulation of decidual NK cell and macrophage function through interactions with killer cell Ig-like receptors and leukocyte Ig-like receptors (8–11) and may promote T cell and endothelial cell apoptosis through $CD8^+$ and CD160-mediated mechanisms (12, 13). In addition, reduced expression of HLA-G in endovascular and interstitial trophoblasts has been noted in pre-eclampsia and intrauterine growth restriction, where impaired trophoblast invasion, placental development, and utero-placental blood flow are thought to contribute to the pathophysiology of these clinical situations (14). However, the in vivo role of HLA-G remains unclear because experimental intervention in early human pregnancy is not feasible. Thus, there is a pressing need for an animal model for the study of HLA-G function.

Comparison with the human MHC class I loci has revealed that the rhesus monkey expresses the products of highly polymorphic *HLA-A*-like and *HLA-B*-like loci (termed *Mamu-A* and *Mamu-B*, for *Macaca mulatta*) (15, 16), and the G locus has also been demonstrated in apes and macaques (17, 18). While we have shown in the rhesus that *Mamu-G* is a pseudogene (17), a novel MHC class I locus, *Mamu-AG,* shares a number of features of *HLA-G* (19). These include low polymorphism and a truncated cytoplasmic domain, alternative splicing (19), the expression of a soluble isoform (20), and a distinctive expression pattern in which the highest mRNA and protein levels are found in placental trophoblasts (21–23). The 25D3 mAb specific for Mamu-AG (23) identified Mamu-AG expression as early as days 14–19 of gestation in rhesus monkey cytotrophoblasts invading the maternal vessels and endometrium, the cytotrophoblasts delineating the maternal-fetal interface, and also the syncytiotrophoblasts (STB)[4] of chorionic villi of the definitive placenta (23). The expression of Mamu-AG at the implantation site within the first week of pregnancy suggests a role in trophoblast invasion and establishment of a unique immunologic microenvironment at the maternal-fetal interface.

The aim of this study was to begin to define an in vivo function for Mamu-AG through anti-Mamu-AG passive immunization in early pregnancy. This report demonstrates that interfering with Mamu-AG on the trophoblast surface negatively affects placental growth and development, as well as decidual differentiation and maturation in the nonhuman primate model, and supports an important role for trophoblast MHC class I expression at the primate maternal-fetal interface.

Materials and Methods

Animals and tissues

Adult female rhesus monkeys (*M. mulatta*) weighing 6.5–9.5 kg and used for timed mating were from the colony maintained at the National Primate Research Center (University of Wisconsin, Madison, WI). All experimental procedures were performed in accordance with the National Institutes of Health Guidelines for Care and Use of Laboratory Animals and

[4]Abbreviations used in this paper: STB, syncytiotrophoblast; 25D3, anti-Mamu-AG mAb; CG, chorionic gonadotropin; DC-SIGN, DC-specific ICAM3-grabbing nonintegrin; EVCT, extravillous cytotrophoblast; IHC, immunohistochemistry; NS, non-specific; VEGF, vascular endothelial growth factor.

with the approval of the University of Wisconsin Graduate School Animal Care and Use Committee.

Rhesus monkey implantation sites were obtained from monkeys undergoing normal pregnancy (untreated control), monkeys treated in vivo with 4 mg of nonspecific (NS) purified $F(ab')_2$ (NS treated), or monkeys treated in vivo with 4 mg of an anti-Mamu-AG (clone 25D3) $F(ab')_2$ (25D3 treated) by i.v. injection (0.5 ml saline) each day from day 18 through day 24 of gestation ($n = 4$ for each group; day 0 = the day after the ovulatory luteinizing hormone peak; day 165 = term). All tissues were treated identically in a standardized manner. Intact uteroplacental units were obtained from animals following perfusion with 2% paraformaldehyde/PBS on day 24 as previously described (23). At least two samples were taken from each placental disc (average normal pregnancy primary disc size was 3.0 × 2.8 × 0.2 cm). Utero-placental tissues were secondarily fixed for 4 h in 2% paraformaldehyde and embedded in paraffin, sectioned (5 μm), deparaffinized in xylene, rehydrated in decreasing ethanol concentrations, and immunostained with selected Abs. For frozen sections, separate samples from the same placentas were fixed in paraformaldehyde followed by cryopreservation by immersion in sucrose and PBS and then frozen, sectioned (5 μm), and stained (21). The selected samples were embedded in paraffin or frozen with the cut face down to meet the requirements for vertical sections, which is necessary for design-based estimation of the surface area (24, 25).

Histological and morphometric analysis

Randomly selected sections of the paraffin-embedded material were stained with H&E. The following morphometric placental parameters were evaluated: mean number of villous cross-sections per mm^2 of paraffin section, percentage of total number of the various villous classes (examined under ×4 objective), length of stem villi, diameter of villi, the thickness of the villous trophoblast, villous surface area, villous stromal area, the number of vessel cross-sections per villus (examined under ×10 objective), maximal luminal diameter of villous vessels, and vessel surface area (examined under ×20 objective) (25–29). Stromal/epithelial surface and vessel/villous surface ratios were calculated.

Decidual tissues were examined and evaluated on the basis of the following morphologic features: changes in the decidual epithelium (epithelial plaque reaction and glandular changes) or decidual stroma (leukocytic infiltration, localized edema, decidualization of stromal cells, and modifications of arteriolar vessels), number of vessel cross-sections per 0.01 μm^2 of decidua, and villous lacunar formation (30–33). Digital images were captured using a Leica DM IRB microscope equipped with an Optronics MagnaFire digital camera and software. Images were taken of slides free of fixation, sectioning, or staining artifacts. Five randomly selected microscopic fields from the central region of each placental specimen were acquired. Morphometric analyses were performed using NIH ImageJ 1.32j software for measuring photomicrograph image features (34) on serial placental sections. Contours of the structurally intact villi and their stroma and vessels were traced manually on the computer monitor with a mouse-controlled cursor at on-screen magnification to calculate the areas of these components (28). The results from five images were averaged to give one value for each specimen (25). All measurements were analyzed blind (without knowledge of

the treatment group) by the same person. Mean ± SEM were calculated for each group and the statistical significance of the differences between pairs of groups was assessed using ANOVA (Vassar Stats) followed by Tukey's Honestly Significant Difference test.

Immunohistochemistry

Paraffin-embedded and frozen sections (5 μm) were stained with Abs and visualized using the Vectastain ABC peroxidase complex kit and Vector NovaRED substrate kit for peroxidase (Vector Laboratories) generally as described previously (23, 35). The Abs used and their working concentrations are given in Table I. Frozen sections of the control group animals (Fig. 1) were stained with the anti-Mamu-AG (clone 25D3) mouse (11.2 μg/ml) mAb. Mouse IgG1, IgG2, or normal rabbit or sheep serum (Sigma-Aldrich) served as negative controls. To confirm the distribution of 25D3 mAb at the implantation site, frozen sections were incubated with the biotinylated anti-mouse IgG (7.5 μg/ml) (Vector Laboratories; Fig. 1). Intravillous and decidual vascular elements were identified by anti-CD31 or anti-IDO Ab staining, respectively. Ki67-stained nuclei were counted in five high power fields (under ×40 objective) and the values were expressed as a percentage of the total cytotrophoblast nuclei counted in fields of view chosen in a systematic random fashion from each placenta (36).

Results

To confirm the distribution of the anti-Mamu-AG 25D3 mAb at the implantation site in passively immunized monkeys, frozen sections were incubated with biotinylated anti-mouse IgG. In 25D3-treated placentas, positive immunohistochemistry (IHC) staining was identified in villous STB (Fig. 1*A*), extravillous cytotrophoblasts (EVCT) of the trophoblastic shell, and the cell columns (Fig. 1*B*). In contrast, there was no positive staining (no mAb attachment) in placental tissue from untreated control (Fig. 1*E*) or NS-treated (Fig. 1*F*) animals. The anti-mouse staining is identical with Mamu-AG distribution (Fig. 1, *C* and *D*), which is expressed in the villous STB (Fig. 1*C*), and the EVCT of proximal columns and the trophoblastic shell delineating the maternal-fetal interface (Fig. 1*D*). These results confirm adequate mAb penetration and binding to endogenous Mamu-AG expressed at the trophoblast surface.

Analysis of placental growth and development

In the rhesus monkey placenta, by days 22–25 of gestation there is extensive branching of the villi, which occurs by longitudinal splitting of the stem villi and cell columns to form groups of parallel branches with a common insertion into the basal plate (type I branches) or by the sprouting of large diameter side branches (type II branches) in the zone nearer the chorionic plate (30) (Fig. 2*A*). The percentages of the various villous types are shown in Table II. The percentages of all villous types in 25D3-treated animals were significantly different from those of both untreated and NS-treated placentas. The only statistically significant difference between untreated and NS-treated animals was a modest difference in total villi (Table II). 25D3-treated placentas showed significantly higher ($p < 0.01$) numbers of stem villi and their type I branches and significantly lower percentages ($p < 0.01$) of type

II branches and floating villi compared with both untreated and NS-treated animals. This suggests a delay in overall placental development.

Morphometric analysis of the chorionic villi revealed discrete deficits in villous growth. The length of stem villi (Fig. 2*B*) and diameter of stem, branching, and floating villi (Fig. 2*C*) were significantly different between 25D3-treated and NS-treated or untreated placentas ($p < 0.01$). In addition, trophoblast thickness (Fig. 2*D*) and the villous stromal/epithelial (i.e., total trophoblast) area ratio (Fig. 2*E*) were significantly decreased by 25D3 treatment. The percentage of Ki67-positive cytotrophoblasts (proliferative index) in placentas from 25D3-treated animals was significantly different ($p < 0.01$) from that of NS-treated and untreated placentas in all villous compartments (Fig. 2, *F* and *G*). Thus, stromal growth as well as trophoblast proliferation was delayed by 25D3 treatments.

Vascularization of chorionic villi

The vascularity of the chorionic villi was evaluated by IHC for CD31 (Fig. 3*A*). The number of vessel cross-sections per villus, in all villous categories, was significantly reduced in floating, type I branching, and stem villi for 25D3 vs NS-treated placentas (Fig. 3*B*), and the mean maximal luminal diameter (26) was reduced by 25D3 treatment in type I branching and floating villi (Fig. 3*C*). The vessel/villous surface ratio of all categories of villi was also reduced in 25D3-treated placentas in comparison with NS-treated placentas (not shown). Because of reduced villous vascularization, we evaluated vascular endothelial growth factor (VEGF) and VEGF receptor (FLT1 and KDR) expression by IHC. Although there was strong positive staining for VEGF and FLT1 in both villous trophoblasts and endothelial cells in all treatment groups (not shown), immunostaining for KDR (Flk-1) in 25D3-treated monkeys was consistently reduced in comparison with untreated and NS-treated placentas (Figs. 3, *D–F*).

Because of this effect on differentiated trophoblast function, we examined chorionic gonadotropin (CG) expression by IHC in monkey placentas (Fig. 4). The staining was similar in untreated and NS-treated placentas: strong positive staining in STB of chorionic villi (Fig. 4*A*). In the 25D3-treated group, CG expression was relatively lower and irregular (Fig. 4*B*).

Lacunar development and endometrial invasion

The lacunae are the intervillous maternal blood spaces that arise as the chorionic villi are formed during weeks 1–2 of rhesus placental development (31). In untreated control and NS-treated placentas (Fig. 5*A*) we observed expanded and unexpanded lacunae with maternal RBC, whereas in the 25D3-treated group only unexpanded lacunae were seen, with little evidence of intervillous maternal blood (Fig. 5*B*).

EVCT gain access to maternal endometrial arterioles soon after blastocyst implantation in higher primates (32, 33). The lumina of small arterioles directly beneath the implantation site were completely or partially occluded by EVCT (identified by cytokeratin staining) in all treatment groups (Figs. 5, *C* and *D*). Invaded vessels had substantial modification of the endothelial layer in all groups of animals, as shown by discontinuous or absent Von Willebrand Factor staining (Figs. 5, *E* and *F*) of the invaded vessels. While EVCT invasion

into the smooth muscle actin-positive tunica medium progressed as expected through gaps in the smooth muscle layer with substantial disruption and removal of the spiral arterial wall in untreated control and NS-treated decidual vessels (Fig. 5*G*), the tunica medium of spiral arterioles in 25D3-treated animals remained intact (Fig. 5*H*).

Decidual leukocyte distribution

The rhesus decidual response to implantation includes an increase in dendritic cell-specific ICAM3-grabbing nonintegrin (DC-SIGN) expression in a subset of macrophages localized to the implantation site, an increase in the number of decidual NK cells, and a decrease in decidual T cells (35, 37). As expected, most of the leukocytes observed in decidual stroma were CD56-positive NK cells and CD68-positive macrophages (Fig. 6*A*). CD68-positive and CD56-positive cells abundantly infiltrated the decidua and were not different among the three groups of animals (Fig. 6*A*). In contrast, DC-SIGN-positive cell abundance in the decidua was clearly lower in specimens collected from monkeys passively immunized with anti-Mamu-AG compared with untreated control and NS-treated groups (Figs. 6*A*, *F*, and *G*). In untreated control and NS-treated groups there were a few isolated CD3-positive cells (Fig. 6*H*), whereas in 25D3-treated animals CD3-positive cells were increased and sometimes formed a dense infiltrate around noninvaded decidual vessels (Fig. 6*I*). In addition, the number of vessels per unit area of decidua also was significantly lower in 25D3-treated animals (Figs. 6, *J* and *K*).

Epithelial plaque and edema

Responses to the presence of the embryo in the outer functional zones of the rhesus endometrium include formation of a luminal epithelial plaque reaction in the immediate vicinity of the implanting embryo and subepithelial edema at the periphery of the plaque. By day 24, most cells of the epithelial plaque undergo degeneration (31, 33). We observed in the NS-treated (Fig. 7*A*) and untreated control (not shown) groups only irregular small patches of degenerating cells remaining at the periphery of the implantation site, located between the cytotrophoblast shell and the decidualizing stroma. At the margin of the plaque, mild subepithelial edema was seen in some areas (Fig. 7*B*). In 25D3-treated monkeys, the epithelial plaque was clearly visible and continuous (Fig. 7*A*) as was extreme subepithelial edema, including blister-like structures adjacent to the placenta (Fig. 7*C*). Thus, 25D3-treated animals exhibited a delayed regression of the plaque reaction.

Stromal decidualization and differentiation of endometrial glands

During decidualization, the endometrial glands initially enlarge and the glandular epithelium actively secretes material into the lumen (27). Untreated and NS-treated animals displayed enlarged, dilated decidual glands with a thin epithelial layer and accumulated secretion in the lumen (Fig. 7*D*). In contrast, restricted dilation of the decidual glands was found in 25D3-treated decidua (Fig. 7*E*).

Under the influence of blastocyst implantation, the transformation of the primate endometrium into the decidua includes differentiation of stromal fibroblasts near the implantation site, with enlargement of endometrial stromal cells showing a rounded or polygonal morphology. In the anti-Mamu-AG treated group, decidualization was rather

patchy, as confirmed by a significant increase in the number of nuclei per unit of stromal area (NS-treated, 169.1 ± 2.1 vs 25D3-treated, 205.4 ± 2.3 nuclei/0.01 mm^2; $p < 0.01$).

Discussion

Rhesus monkeys in the second week postimplantation were passively immunized with a mAb against the placental MHC class I molecule Mamu-AG. There were broad effects of passive immunization on placental development as well as morphological responses in the maternal decidua. Evaluation of growth and proliferation within the chorionic villi, as well as the number and the diameter of fetal blood vessels within villi, indicated an overall delay in placental development. These results were mirrored within the decidual compartment where a broad spectrum of functional parameters were likewise inhibited or delayed, including the remodeling of maternal spiral arterioles by invasive extravillous trophoblasts, the expression of DC-SIGN in decidual macrophages, the displacement of T cells from the functional endometrium, and the differentiation of decidual stromal fibroblasts and the endometrial glandular epithelium. These data suggest an important role for MHC class I molecules expressed on primate trophoblasts in establishing an environment for pregnancy success through a coordinated set of interactions between the placenta and decidual tissues. Although there have been numerous studies evaluating HLA-G action in vitro, its biological function has remained exceedingly difficult to study in the in vivo setting. The significant outcomes of this study illustrate the useful applications of the passive immunization paradigm in primate experimental models.

A substantial majority of the leukocytes in the human and the rhesus monkey decidua of early pregnancy are NK cells, with the balance primarily macrophages and some $CD8^+$ T cells (33, 35, 38, 39). The distinct decidual NK cell phenotype (bright CD56 expression and reduced CD16 levels, angiogenic factor, adhesion, and chemotactic factor gene expression) (40) supports an important function for decidual NK cells in pregnancy establishment distinct from peripheral blood NK cell function. Indeed, recent studies have demonstrated that decidual NK may have important roles in promoting trophoblast invasion (41) and decidual vascular remodeling (42) in human pregnancy. In human pathological pregnancies, there have been reports from several groups that the diminished invasion of maternal spiral arteries by endovascular extravillous human trophoblasts is associated with reduced HLA-G expression in the extravillous trophoblasts and a decrease in the expected loss of vascular smooth muscle (14, 43). Thus, an experimental reduction in Mamu-AG might be predicted to result in decreased endothelial and/or smooth muscle removal. This prediction was partially borne out by the results of anti-Mamu-AG passive immunization with regard to changes in vascular smooth muscle in maternal spiral arteries. Although our studies did not reveal changes in the appearance of endovascular rhesus trophoblasts, there was a consistent interruption of subsequent trophoblast remodeling of these invaded vessels. Although this suggests that Mamu-AG may have no role in any interactions with maternal leukocytes that may influence trophoblast migration (such as chemotactic factor secretion; Ref. 41), alternatively the rhesus monkey may have concluded a substantial portion of endovascular trophoblast invasion in the initial ~11 days postimplantation, before we initiated Ab treatment on day 18 of gestation. The differential control of endovascular migration of extravillous trophoblasts vs the breaching of the vascular smooth muscle of those vessels is

not understood. Further study of the sequelae of this early placental insult in the rhesus may allow the development of primate preclinical models of implantation defects and placental insufficiency.

Although the roles of resident macrophages and T cells in the primate decidua are less extensively studied, macrophages in particular seem ideally poised to respond to implantation as they are localized in close association with the maternal spiral arteries in both human (44) and rhesus (35, 37) implantation. Indeed, studies with soluble HLA-G and macrophage-like cell lines or $CD8^+$ T cells have suggested that these cells may also be direct targets of HLA-G action (45, 46). It has been previously reported that macrophages can effect vascular smooth muscle apoptosis, like trophoblasts (45–47), through Fas/FasL-mediated mechanisms (48). In this regard, the close localization of macrophages in the rhesus to the spiral arteries invaded by trophoblasts (37) may be of particular significance. It was intriguing that the pregnancy-specific induction of DC-SIGN we have previously noted in a subset of decidual macrophages in rhesus decidua (35) in response to implantation was significantly limited by passive immunization against Mamu-AG. Failure to ligate Mamu-AG receptors and activate the pregnancy response in macrophages may contribute to the interruption of normal vessel modification. This was not an effect on overall macrophage survival, because total macrophage numbers did not change with passive immunization. Thus, pregnancy-specific differentiation is an important area for further study. Because CG expression in the rhesus placenta is apparently decreased or inconsistent, this may also provide a mechanism by which decidual maturation is delayed.

An unexpected outcome of passive immunization against Mamu-AG was the significant effect on placental growth and vascularization. One interpretation of these results is that Mamu-AG neutralization abrogates its effects on a different target cell (e.g., decidual NK cells) to the detriment of placental development. This could be due to changes in decidual growth factor or cytokine secretion, because numerous soluble factors secreted by leukocytes may affect placental growth and development. It is also possible that, in the absence of Mamu-AG signaling, expression of decidual factor(s) inhibits placental development. Alternatively, loss of angiogenic factor production by uterine NK cells may limit uteroplacental blood flow and early growth of the placenta. It is possible that ligation of Mamu-AG by 25D3 in the villous syncytiotrophoblast apical membranes disrupts membrane trafficking or protein-protein interactions along the syncytial surface, altering the dialogue between the syncytiotrophoblasts, villous cytotrophoblasts, and the villous mesenchyme. Further studies targeting decidual leukocytes or other syncytial surface Ags can address these alternative interpretations.

Although the present study has revealed important effects of anti-Mamu-AG passive immunization on rhesus pregnancy, there are several important questions that remain to be addressed. Despite the scope of the changes observed in the deciduae, it may be that only a subset of the effects are due to a direct interaction between the invasive endovascular trophoblasts and decidual cells. Owing to a relatively low level of interstitial invasion into the rhesus decidua, effects on decidual differentiation, subepithelial edema, endometrial plaque degeneration, and endometrial gland transformation may be more easily explained by changes in placental/decidual soluble regulatory factors. As with HLA-G, the soluble

isoform of Mamu-AG (20) may be considered a candidate for wider distribution throughout the decidua adjacent to the trophoblastic shell. Soluble HLA-G has been shown to promote T cell (12) and endothelial cell apoptosis (13), as well as influence gene expression in macrophage-like U937 cells (49). Soluble Mamu-AG present in the decidual space would be available for interaction with decidual NK cell receptors, as well as possibly endometrial T cells and macrophages and vascular smooth muscle. Importantly, decidual NK cells are the most abundant cells in the decidua throughout pregnancy and are well-positioned for influencing decidual maturation. Because NK cell depletion in the mouse decidua interrupts vascularization (50), a harmonizing role for NK cells in both hemochorial species is attractive despite the lack of evidence that placental MHC has a role in the modulation of maternal decidual leukocytes in the mouse. It is also possible that effects of passive immunization on other placental factors, including CG (51), contribute to the decidual changes observed.

In addition, the physiological sequelae of this early insult in placental development and decidual maturation on the outcome of pregnancy in terms of maternal and fetal well-being, particularly neonatal health, are not known. In human pregnancy, abnormal or inadequate implantation and placental growth and development are associated with decreased or suboptimal HLA-G expression in extravillous trophoblasts (14, 43). The ability to directly examine prenatal and postnatal sequelae of interference with placental MHC class I signaling to maternal immune cells and other possible targets at the maternal-fetal interface in the rhesus is an important advance in establishing a primate model highly homologous to human placental, decidual, immune, and fetal morphology and function.

Acknowledgments

We thank the Veterinary, Pathology, and Reproductive Services staff of the Wisconsin National Primate Research Center for all procedures with animals, Fritz Wegner in Wisconsin National Primate Research Center Assay Services for hormone assays to confirm ovulation and pregnancy, and Ju-dith Peterson for assistance in preparation of this manuscript.

References

1. McMaster MT, Librach CL, Zhou Y, Lim KH, Janatpour MJ, DeMars R, Kovats S, Damsky C, Fisher SJ. Human placental HLA-G expression is restricted to differentiated cytotrophoblasts. J Immunol. 1995; 154:3771–3778. [PubMed: 7706718]
2. Hunt JS. Stranger in a strange land. Immunol Rev. 2006; 213:36–47. [PubMed: 16972895]
3. Blaschitz A, Hutter H, Dohr G. HLA class I protein expression in the human placenta. Early Pregnancy. 2001; 5:67–69. [PubMed: 11753519]
4. Clements CS, Kjer-Nielsen L, Kostenko L, Hoare HL, Dunstone MA, Moses E, Freed K, Brooks AG, Rossjohn J, McCluskey J. Crystal structure of HLA-G: a nonclassical MHC class I molecule expressed at the fetal-maternal interface. Proc Natl Acad Sci USA. 2005; 102:3360–3365. [PubMed: 15718280]
5. Sanders SK, Giblin PA, Kavathas P. Cell-cell adhesion mediated by CD8 and human histocompatibility leukocyte antigen G, a nonclassical major histocompatibility complex class I molecule on cytotrophoblasts. J Exp Med. 1991; 174:737–740. [PubMed: 1908512]
6. Lee N, Malacko AR, Ishitani A, Chen MC, Bajorath J, Marquardt H, Geraghty DE. The membrane-bound and soluble forms of HLA-G bind identical sets of endogenous peptides but differ with respect to TAP association. Immunity. 1995; 3:591–600. [PubMed: 7584149]

7. Diehl M, Munz C, Keilholz W, Stevanovic S, Holmes N, Loke YW, Rammensee HG. Nonclassical HLA-G molecules are classical peptide presenters. Curr Biol. 1996; 6:305–314. [PubMed: 8805247]
8. Colonna M, Nakajima H, Navarro F, Lopez-Botet M. A novel family of Ig-like receptors for HLA class I molecules that modulate function of lymphoid and myeloid cells. J Leukocyte Biol. 1999; 66:375–381. [PubMed: 10496306]
9. Navarro F, Llano M, Bellon T, Colonna M, Geraghty DE, Lopez-Botet M. The ILT2(LIR1) and CD94/NKG2A NK cell receptors respectively recognize HLA-G1 and HLA-E molecules co-expressed on target cells. Eur J Immunol. 1999; 29:277–283. [PubMed: 9933109]
10. Shiroishi M, Tsumoto K, Amano K, Shirakihara Y, Colonna M, Braud VM, Allan DS, Makadzange A, Rowland-Jones S, Willcox B, et al. Human inhibitory receptors Ig-like transcript 2 (ILT2) and ILT4 compete with CD8 for MHC class I binding and bind preferentially to HLA-G. Proc Natl Acad Sci USA. 2003; 100:8856–8861. [PubMed: 12853576]
11. Rajagopalan S, Bryceson YT, Kuppusamy SP, Geraghty DE, van der Meer A, Joosten I, Long EO. Activation of NK cells by an endocytosed receptor for soluble HLA-G. PloS Biol. 2006; 4:e9. [PubMed: 16366734]
12. Fournel S, Aguerre-Girr M, Huc X, Lenfant F, Alam A, Toubert A, Bensussan A, Le Bouteiller P. Cutting edge: soluble HLA-G1 triggers CD95/CD95 ligand-mediated apoptosis in activated $CD8^+$ cells by interacting with CD8. J Immunol. 2000; 164:6100–6104. [PubMed: 10843658]
13. Fons P, Chabot S, Cartwright JE, Lenfant F, L'Faqihi F, Giustiniani J, Herault JP, Gueguen G, Bono F, Savi P, et al. Soluble HLA-G1 inhibits angiogenesis through an apoptotic pathway and by direct binding to CD160 receptor expressed by endothelial cells. Blood. 2006; 108:2608–2615. [PubMed: 16809620]
14. Le Bouteiller P, Pizzato N, Barakonyi A, Solier C. HLA-G, pre-eclampsia, immunity and vascular events. J Reprod Immunol. 2003; 59:219–234. [PubMed: 12896824]
15. Watkins DI. The evolution of major histocompatibility class I genes in primates. Crit Rev Immunol. 1995; 15:1–29. [PubMed: 8519421]
16. Adams EJ, Parham P. Species-specific evolution of MHC class I genes in the higher primates. Immunol Rev. 2001; 183:41–64. [PubMed: 11782246]
17. Boyson JE, Iwanaga KK, Golos TG, Watkins DI. Identification of the rhesus monkey HLA-G ortholog: mamu-G is a pseudogene. J Immunol. 1996; 157:5428–5437. [PubMed: 8955191]
18. Arnaiz-Villena A, Morales P, Gomez-Casado E, Castro MJ, Varela P, Rojo-Amigo R, Martinez-Laso J. Evolution of MHC-G in primates: a different kind of molecule for each group of species. J Reprod Immunol. 1999; 43:111–125. [PubMed: 10479048]
19. Boyson JE, Iwanaga KK, Golos TG, Watkins DI. Identification of a novel MHC class I gene: *mamu-AG*, expressed in the placenta of a primate with an inactivated G locus. J Immunol. 1997; 159:3311–3321. [PubMed: 9317129]
20. Ryan AF, Grendell RL, Geraghty DE, Golos TG. A soluble isoform of the rhesus monkey nonclassical MHC class I molecule mamu-AG is expressed in the placenta and the testis. J Immunol. 2002; 169:673–683. [PubMed: 12097369]
21. Slukvin II, Boyson JE, Watkins DI, Golos TG. The rhesus monkey analogue of human lymphocyte antigen-G is expressed primarily in villous syncytiotrophoblast. Biol Reprod. 1998; 58:728–738. [PubMed: 9510960]
22. Slukvin II, Watkins DI, Golos TG. Tissue distribution of the mRNA for a rhesus monkey major histocompatibility class Ib molecule, mamu-AG. Tissue Antigens. 1999; 53:282–291. [PubMed: 10203022]
23. Slukvin II, Lunn DP, Watkins DI, Golos TG. Placental expression of the nonclassical MHC class I molecule Mamu-AG at implantation in the rhesus monkey. Proc Natl Acad Sci USA. 2000; 97:9104–9109. [PubMed: 10922066]
24. Baddeley AJ, Gundersen HJ, Cruz-Orive LM. Estimation of surface area from vertical sections. J Microsc. 1986; 142:259–276. [PubMed: 3735415]
25. Maly A, Goshen G, Sela J, Pinelis A, Stark M, Maly B. Histomorphometric study of placental villi vascular volume in toxemia and diabetes. Hum Pathol. 2005; 36:1074–1079. [PubMed: 16226106]
26. Willemse F, Nap M, de Bruijn HW, Hollema H. Quantification of vascular density and of lumen and vessel morphology in endometrial carcinoma: evaluation of their relation to serum levels of

tissue polypeptide-specific antigen and CA-125. Anal Quant Cytol Histol. 1997; 19:1–7. [PubMed: 9051179]

27. Benirschke K, Kaufmann P. The Pathology of the Human Placenta. 4. Springer-Verlag; New York: 2000.
28. Chen CP, Bajoria R, Aplin JD. Decreased vascularization and cell proliferation in placentas of intrauterine growth-restricted fetuses with abnormal umbilical artery flow velocity waveforms. Am J Obstet Gynecol. 2002; 187:764–769. [PubMed: 12237661]
29. Mayhew TM, Ohadike C, Baker PN, Crocker IP, Mitchell C, Ong SS. Stereological investigation of placental morphology in pregnancies complicated by pre-eclampsia with and without intrauterine growth restriction. Placenta. 2003; 24:219–226. [PubMed: 12566249]
30. King BF, Mais JJ. Developmental changes in rhesus monkey placental villi and cell columns: scanning electron microscopy. Anat Embryol. 1982; 165:361–376. [PubMed: 7158818]
31. Enders AC. Trophoblast differentiation during the transition from trophoblastic plate to lacunar stage of implantation in the rhesus monkey and human. Am J Anat. 1989; 186:85–98. [PubMed: 2782290]
32. Blankenship TN, Enders AC. Trophoblast cell-mediated modifications to uterine spiral arteries during early gestation in the macaque. Acta Anat. 1997; 158:227–236. [PubMed: 9416353]
33. Enders AC, Welsh AO, Schlafke S. Implantation in the rhesus monkey: endometrial response. Am J Anat. 1985; 173:147–169. [PubMed: 20726118]
34. Lau D, Seibert A, Gandara D, Laptalo L, Geraghty E, Coulon C. Computer-assisted image analysis bronchioloalveolar carcinoma. Clin Lung Cancer. 2005; 6:281–286. [PubMed: 15845178]
35. Breburda EE, Dambaeva SV, Slukvin II, Golos TG. Selective distribution and pregnancy-specific expression of DC-SIGN at the maternal-fetal interface in the rhesus macaque: DC-SIGN is a putative marker of the recognition of pregnancy. Placenta. 2006; 27:11–21. [PubMed: 16310033]
36. Babischkin JS, Burleigh DW, Mayhew TM, Pepe GJ, Albrecht ED. Developmental regulation of morphological differentiation of placental villous trophoblast in the baboon. Placenta. 2001; 22:276–283. [PubMed: 11286563]
37. Slukvin II, Breburda EE, Golos TG. Dynamic changes in primate endometrial leukocyte populations: differential distribution of macrophages and natural killer cells at the rhesus monkey implantation site and in early pregnancy. Placenta. 2004; 25:297–307. [PubMed: 15028422]
38. Tabiasco J, Rabot M, Aguerre-Girr M, El Costa H, Berrebi A, Parant O, Laskarin G, Juretic K, Bensussan A, Rukavina D, Le Bouteiller P. Human decidual NK cells: unique phenotype and functional properties, a review. Placenta. 2006; 27(Suppl A):S34–S39. [PubMed: 16516963]
39. Slukvin II, Watkins DI, Golos TG. Phenotypic and functional characterization of rhesus monkey decidual lymphocytes: rhesus decidual large granular lymphocytes express CD56 and have cytolitic activity. J Reprod Immunol. 2001; 50:57–79. [PubMed: 11254941]
40. Koopman LA, Kopcow HD, Rybalov B, Boyson JE, Orange JS, Schatz F, Masch R, Lockwood CJ, Schachter AD, Park PJ, Strominger JL. Human decidual natural killer cells are a unique NK cell subset with immunomodulatory potential. J Exp Med. 2003; 198:1201–1212. [PubMed: 14568979]
41. Hanna J, Goldman-Wohl D, Hamani Y, Avraham I, Greenfield C, Natanson-Yaron S, Prus D, Cohen-Daniel L, Arnon TI, Manaster I, et al. Decidual NK cells regulate key developmental processes at the human fetal-maternal interface. Nat Med. 2006; 12:1065–1074. [PubMed: 16892062]
42. Lash GE, Schiessl B, Kirkley M, Innes BA, Cooper A, Searle RF, Robson SC, Bulmer JN. Expression of angiogenic growth factors by uterine natural killer cells during early pregnancy. J Leukocyte Biol. 2006; 80:572–580. [PubMed: 16816146]
43. Goldman-Wohl DS, Ariel I, Greenfield C, Hochner-Celnikier D, Cross J, Fisher S, Yagel S. Lack of human leukocyte antigen-G expression in extravillous trophoblasts is associated with pre-eclampsia. Mol Hum Reprod. 2000; 6:88–95. [PubMed: 10611266]
44. Vince GS, Johnson PM. Leucocyte populations and cytokine regulation in human uteroplacental tissues. Biochem Soc Trans. 2000; 28:191–195. [PubMed: 10816125]

45. Harris LK, Keogh RJ, Wareing M, Baker PN, Cartwright JE, Aplin JD, Whitley GS. Invasive trophoblasts stimulate vascular smooth muscle cell apoptosis by a fas ligand-dependent mechanism. Am J Pathol. 2006; 169:1863–1874. [PubMed: 17071607]

46. Bahri R, Hirsch F, Josse A, Rouas-Freiss N, Bidere N, Vasquez A, Carosella ED, Charpentier B, Durrbach A. Soluble HLA-G inhibits cell cycle progression in human alloreactive T lymphocytes. J Immunol. 2006; 176:1331–1339. [PubMed: 16424159]

47. Red-Horse K, Rivera J, Schanz A, Zhou Y, Winn V, Kapidzic M, Maltepe E, Okazaki K, Kochman R, Vo KC, et al. Cytotrophoblast induction of arterial apoptosis and lymphangiogenesis in an in vivo model of human placentation. J Clin Invest. 2006; 116:2643–2652. [PubMed: 16998586]

48. Imanishi T, Han DK, Hofstra L, Hano T, Nishio I, Liles WC, Gown AM, Schwartz SM. Apoptosis of vascular smooth muscle cells is induced by Fas ligand derived from monocytes/macrophage. Atherosclerosis. 2002; 161:143–151. [PubMed: 11882326]

49. McIntire RH, Morales PJ, Petroff MG, Colonna M, Hunt JS. Recombinant HLA-G5 and -G6 drive U937 myelomonocytic cell production of TGF-β1. J Leukocyte Biol. 2004; 76:1220–1228. [PubMed: 15459235]

50. Ashkar AA, Di Santo JP, Croy BA. Interferon γ contributes to initiation of uterine vascular modification, decidual integrity, and uterine natural killer cell maturation during normal murine pregnancy. J Exp Med. 2000; 192:259–270. [PubMed: 10899912]

51. Fazleabas AT, Kim JJ, Strakova Z. Implantation: embryonic signals and the modulation of the uterine environment: a review. Placenta. 2004; 25(Suppl A):S26–S31. [PubMed: 15033303]

52. Matteri RL, Roser JF, Baldwin DM, Lipovetsky V, Papkoff H. Characterization of a monoclonal antibody which detects luteinizing hormone from diverse mammalian species. Domest Anim Endocrinol. 1987; 4:157–165. [PubMed: 3507889]

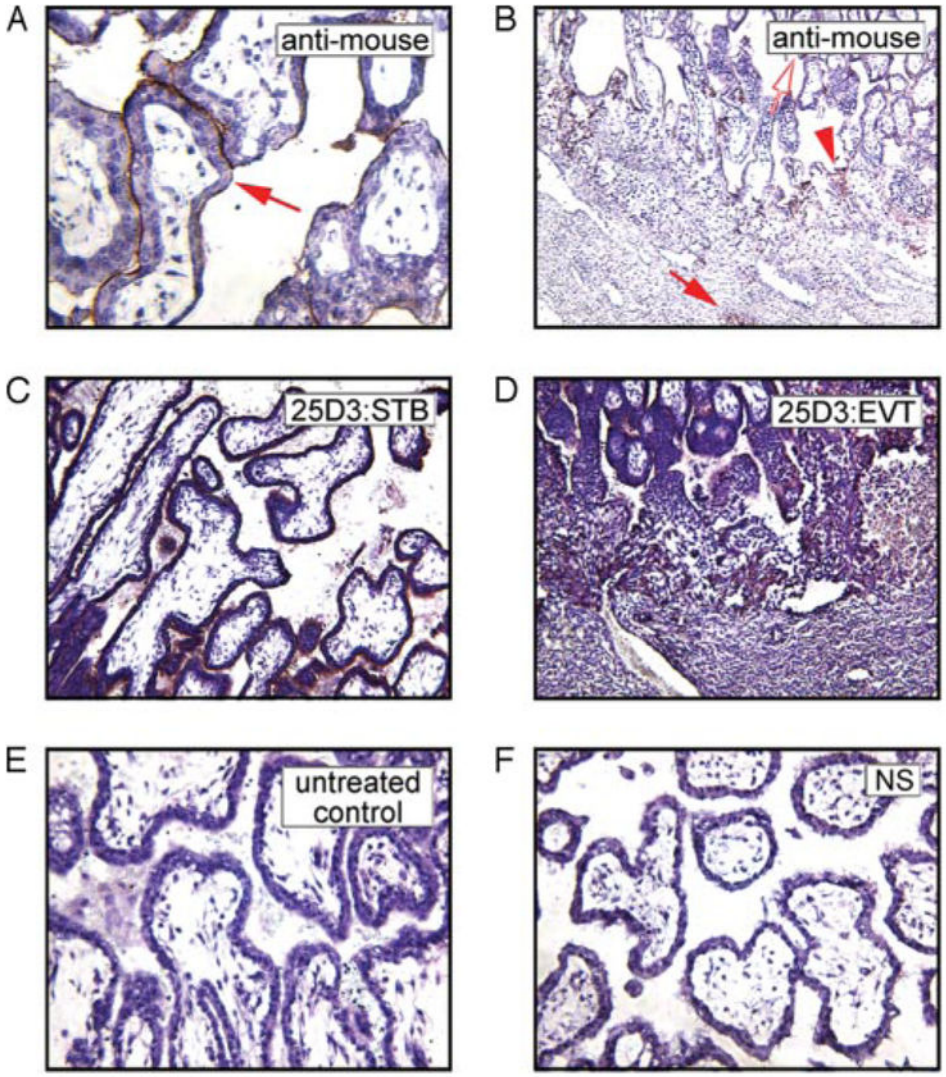

FIGURE 1.

Localization of anti-Mamu-AG (25D3) mAb in passively immunized monkeys. The mAb distribution in the rhesus monkey placenta at the implantation site in villous (*A*) and extravillous (*B*) trophoblasts visualized with anti-mouse IgG in the rhesus monkey placenta is similar to Mamu-AG expression detected in frozen sections with the 25D3 mAb in villous (*C*) and in extravillous (*D*) trophoblasts on day 24 in untreated control pregnancy. Untreated control (*E*) and NS-treated (*F*) groups demonstrated no mAb deposition as detected by immunostaining with a horse anti-mouse IgG.

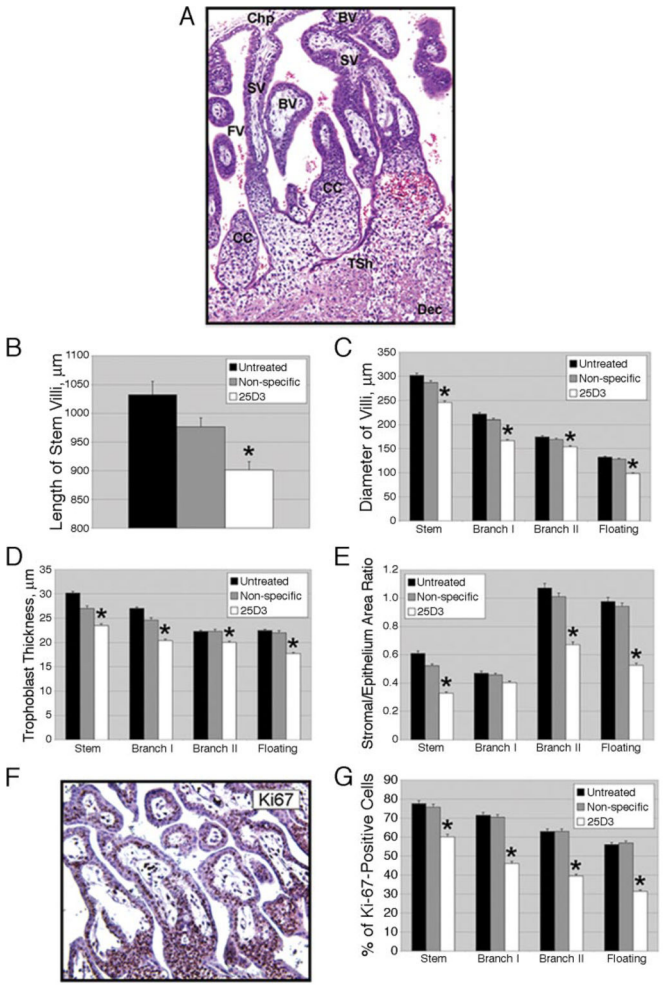

FIGURE 2.

Effects of passive immunization against Mamu-AG on placental growth and morphogenesis. *A*, Depiction of various villous types in the rhesus monkey placenta (untreated control, H&E staining). SV, Stem villus; BV, branching villus; CC, cytotrophoblast column; FV, floating villus; Chp, chorionic plate; Tsh, trophoblastic shell; Dec, decidua. *B*, Length of stem villi in untreated control, NS-treated, or 25D3-treated placentas. The mean + SEM of five independent samples from four placentas per group is shown; *, $p < 0.01$ compared with control groups in this and all other graphs in this figure. *C*, Diameter of classes of villi. *D*, Trophoblast thickness as determined from measurements on five villi in each class within each animal. *E*, Ratios of villous stromal area/trophoblast area. *F*, Representative IHC for Ki67. *G*, Proliferation index (percentage of Ki67-positive trophoblast nuclei) in each villous class.

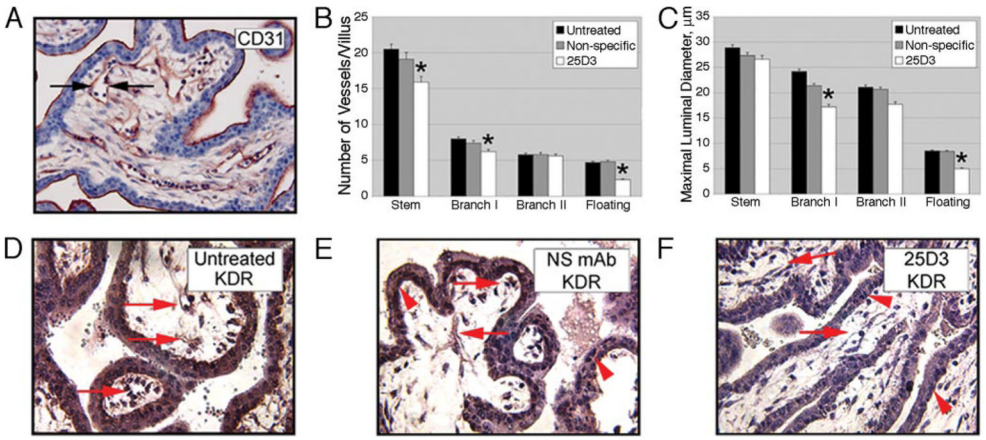

FIGURE 3.

Effects of passive immunization against Mamu-AG on placental vascularization. *A*, Representative IHC for CD31 to visualize villous stromal vessels. *B*, The number of vessels per villus. *C*, Maximal luminal vessel diameter (μm) in individual villous classes (see arrows in *A*).*, $p < 0.01$ in *B* and *C*. *D–F*, Representative IHC for KDR in untreated (*D*), NS-treated (*E*), or 25D3-treated (*F*) animals. Arrows indicate stromal endothelial cells and arrowheads indicate villous cytotrophoblasts.

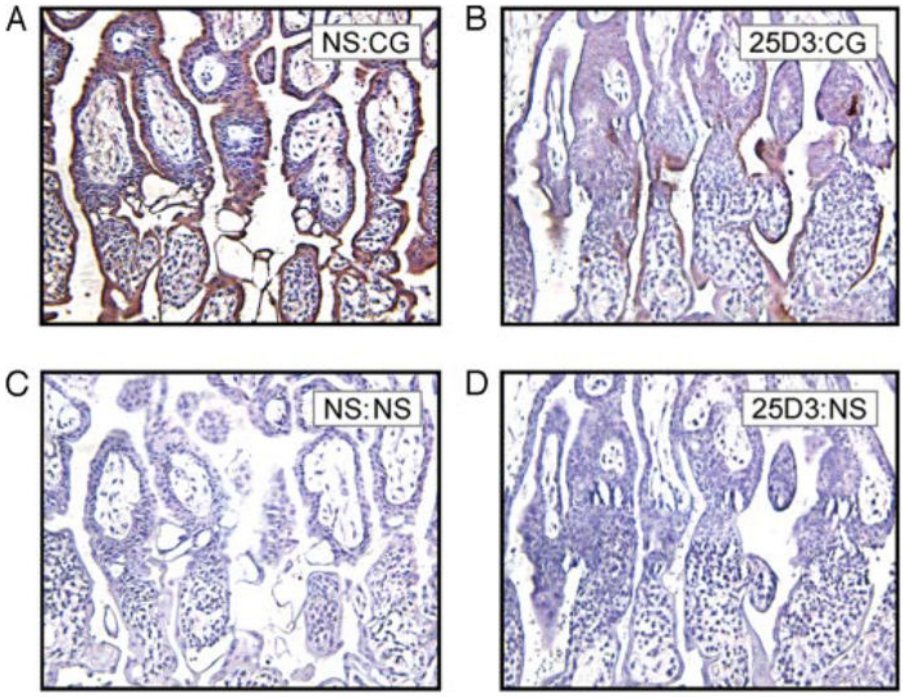

FIGURE 4.

IHC for monkey CG. Rhesus monkey placentas on day 24 of gestation, NS treated (*A* and *C*) or 25D3 treated (*B* and *D*), are shown. Immunostaining was performed on paraffin-embedded sections with anti-CG mAb (*A* and *B*) or a negative control primary Ab (*C* and *D*).

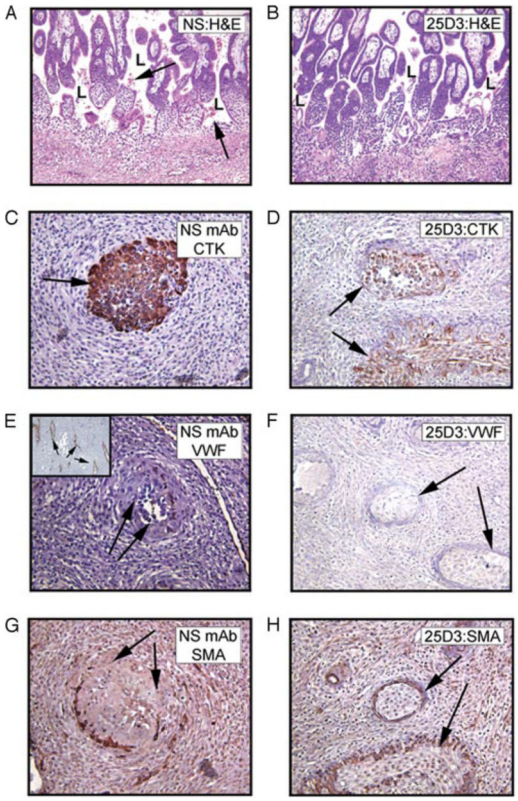

FIGURE 5.

Effect of passive immunization on placental-decidual interactions. Placental lacunae in NS-treated (*A*) or 25D3-treated (*B*) monkeys. Paraffin-embedded sections with H&E staining are shown. Maternal RBC in *A* are indicated by arrows. Lacunae (L) at the placental-decidual border are indicated. *C–H*, Endovascular invasion of placental arterioles by EVCT. Nonspecific treated (*C*, *E*, and *G*) or 25D3-treated (*D*, *F*, and *H*) paraffin-embedded sections were immunostained with the indicated Abs as follows: anti-cytokeratin (CTK) (*C* and *D*; arrows indicate CTK-positive endovascular cytotrophoblasts); anti-von Willebrand factor (VWF) (*E* and *F*; arrows demonstrate lack of positive endothelial cells; see *E*, *inset*, for positively stained endometrial vessels); anti-smooth muscle actin (SMA) (*G* and *H*; arrows indicate discontinuous smooth muscle layer in NS-treated tissue (*G*) or intact smooth muscle layer in 25D3-treated tissue (*H*)).

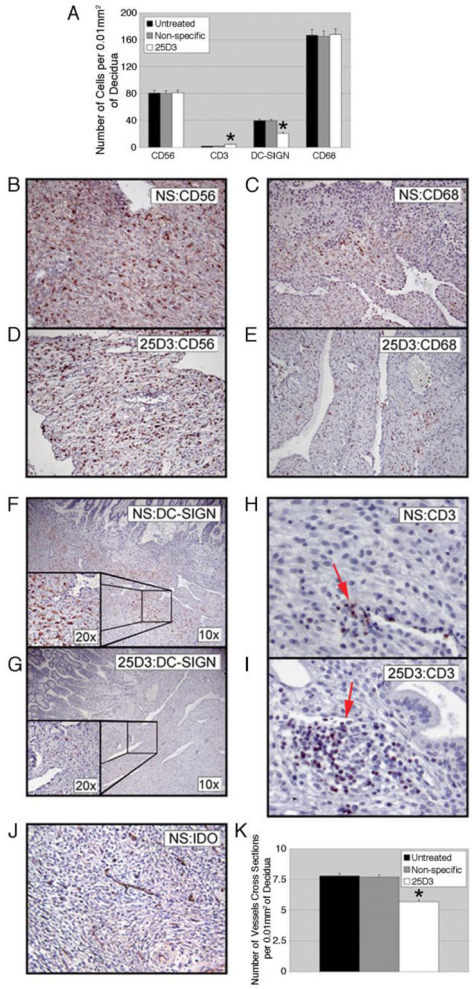

FIGURE 6.

Effects of passive immunization on decidual leukocytes and vascularization. Representative IHC for CD56 (*B* and *D*), CD68 (*C* and *E*), DC-SIGN (*F* and *G*), and CD3 (*H* and *I*) expression in the decidua are shown. Nonspecific treated (*B*, *C*, *F*, *H*, and *J*), and 25D3-treated (*D*, *E*, *G*, and *I*) tissues are shown. *A*, Quantitation of the indicated cell populations in five fields from each of four implantation sites per group. *, $p < 0.01$, indicating 25D3-treated groups that are significantly different from untreated or nonspecific treated animals. *J*, Representative IDO IHC for decidual vessels. *K*, Quantitation of the number of decidual vessels from five random fields of four animals per group.

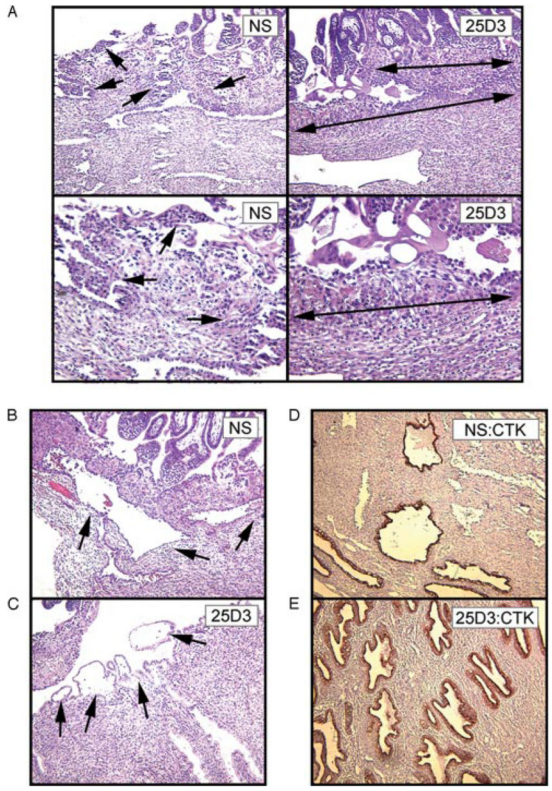

FIGURE 7.

Endometrial responses to passive immunization. *A–C*, Epithelial plaque reaction (*A*) and edema (*B* and *C*) at the margin of the rhesus monkey implantation site in NS specific-treated or 25D3-treated groups; H&E staining of paraffin sections is shown. Broad arrows in *A* delineate the zone of a persistent plaque reaction. *D* and *E*, Endometrial glands in the decidua of NS-treated (*D*) or 25D3-treated (*E*) animals. Paraffin-embedded sections were immunostained with anti-cytokeratin mAb (CTK).

Table I

Ab for immunohistochemistry

Antibody	Source	Working Concentration
Anti-cytokeratin mouse mAb (CAM 5.2)	BD Pharmingen	1 μg/ml
Anti-human smooth muscle actin (SMA) mouse mAb	DakoCytomation	1.7 μg/ml
Anti-VEGF rabbit polyclonal Ab	Santa Cruz Biotechnology	4 μg/ml
Rabbit anti-Flt (VEGFR1)	Santa Cruz Biotechnology	4 μg/ml
Anti-bovine luteinizing hormone (CG) mouse mAB 518B7	J. Roser, University of California, Davis, CA (Ref. 52)	2.5 μg/ml
Sheep anti-IDO	Serotec	27.1 μg/ml
Anti-KDR (VEGFR2/Flk-1) mouse mAb	Research Diagnostics Inc.	2 μg/ml
Anti-human Von Willebrand factor mouse mAb	DakoCytomation	4.8 μg/ml
Anti-Ki-67 mouse mAb	Vector Laboratories	0.75 μg/ml
Anti-CD3 rabbit polyclonal Ab	DakoCytomation	0.75 μg/ml
Anti-CD56 mouse mAb	BD Pharmingen	1.25 μg/ml
Anti-CD68 mouse mAb	DakoCytomation	3.1 μg/ml
Anti-DC-SIGN mouse mAb	BD Pharmingen	0.625 μg/ml

Table II

Number of villous cross-sections and percentage of the various villous types in each treatment group[a]

				Comparisons[b]		
Type of Villi	**Untreated Control**	**Nonspecific Treated**	**25D3 Treated**	**1**	**2**	**3**
Total villi/mm^2	21.0 (0.3)	24.9 (0.9)	31.9 (0.7)	**	**	**
Stem	12.2 (0.1)	12.4 (0.2)	15.6 (0.2)	NS	**	**
Branching type I	23.7 (0.3)	23.2 (0.4)	30.7 (0.2)	NS	**	**
Branching type II	28.6 (0.3)	29.0 (0.2)	24.2 (0.4)	NS	**	**
Floating	35.5 (0.5)	35.5 (0.6)	29.5 (0.2)	NS	**	**

[a] Means (SEM) are presented.

[b] Column 1, comparison of untreated control and NS-treated groups; column 2, comparison of untreated control and 25D3-treated groups; column 3, comparison of NS-treated and 25D3-treated groups. NS, Not statistically significant;

** $p < 0.01$.